ACI STRUCTURAL JOURNAL TECHNICAL PAPER

Title no. 104-S71

Experimental Verification of Strut-and-Tie Model Design Method

by M. Tyler Ley, Kyle A. Riding, Widianto, Sungjin Bae, and John E. Breen

Strut-and-tie models (STM) are a valuable tool for the design of irregular concrete members. This paper presents the experimental results of tests conducted on small-scale, simply supported dapped beams with openings under the load. The design of each test specimen was developed by independent student teams using the ACI 318-05 provisions for STM. An unreinforced specimen was also constructed for comparison. Each reinforced specimen resisted loads greater than the factored design load and exhibited little distress at service load levels. Examination of the behavior of each model permits appraisal of the design model used by each design team. These results show the STM to be a conservative, lower-bound design approach that allows the designer a great deal of flexibility.

Keywords: bearings; size effect; strut-and-tie modeling.

INTRODUCTION

There are limitations in the use of beam theory and classical sectional analysis in the design of concrete structures. These typical design techniques often do not yield meaningful results in areas where there is a change in cross section or loading. These regions are often referred to as D-regions or disturbed regions (Schlaich et al. 1987). D-regions can be analyzed by using strut-and-tie models (STM). In theory, STM provide safe, lower-bound designs (Schlaich et al. 1987; Muttoni et al. 1997). There have not, however, been a large number of experimental validations of this theory.

The relatively few tests on STM have been done on small specimens to allow for easy handling in the testing laboratory. Testing has shown that as size goes up, specimen strength goes down. The fracture mechanics theory has been used to help explain the observed size effect on strength. Smaller structures consume proportionally more energy in the fracture process zone than larger specimens, giving the structure a higher load-carrying capacity relative to the scale factor (Shah et al. 1995). Testing of different size STM specimens would give more confidence in the design method as related to large, real-world structures.

This study presents the results from two series of testing. In the first testing series, six specimens having different reinforcing designs but the same overall geometry and loading pattern were tested. In the second phase of testing, two larger specimens were tested to investigate the size effect on STM tests. The first series of beams in the study were 1:10.5 scaled versions of an example problem from ACI SP-208, "Examples for the Design of Structural Concrete with Strut-and-Tie Models," (Reineck 2002). The larger specimens were a 1:6 scaled model.

The designs used in the first phase of testing were created by five groups of graduate students working independently and in competition to find the steel reinforcing design that had the highest ratio of member failure load to steel cage weight while also providing a deflection of at least $L/100$ at failure under the load point. These results give insight into the design of STM while ensuring safety. Because of the varied requirements, different design approaches were used that emphasized one aspect of performance over another. Despite these differences in design approaches, the failure mechanisms for the specimens were largely similar. A sixth specimen was tested with no reinforcing to find the capacity and cracking pattern of the member only using the tensile strength of the concrete. All designs used the provisions for strut-and-tie modeling in the ACI 318-05 building code (ACI Committee 318 2005). The two specimens in the second phase of testing repeated two of the original six tests but at a larger scale to see the effect of scale.

RESEARCH SIGNIFICANCE

Strut-and-tie modeling is a valuable tool for the design of complex or unusual structural concrete members. Whereas there is a significant amount of literature on strut-and-tie modeling, little experimental validation of the theory has been performed. Efficiency of design, iterative improvement of load-carrying capacity, STM that focus on ductility, and scaling of specimen size are also addressed in the paper. The applicable provisions of the ACI 318-05 building code (ACI Committee 318 2005) were used for all designs except, of course, the unreinforced specimens. The successful set of tests provides experimental verification of the application of strut-and-tie modeling.

EXPERIMENTAL PROGRAM

Phase I testing

Test specimens—The specimens for Phase I testing consisted of six 1:10.5 scale beam specimens from Example Problem 4 of ACI SP-208 (Reineck 2002), as shown in Fig. 1(a). Each specimen measured 1143 mm (45 in.) long, 534 mm (21 in.) high, and 38 mm (1.5 in.) thick. Two geometric irregularities have been introduced into the specimen, which makes the entire specimen a D-region. The first irregularity is a dap that was 1/3 the length and 2/5 the height (368 x 216 mm [14.5 x 8.5 in.]). The second irregularity was a large opening just underneath the load that is 1/3 the length and 1/3 the height of the beam (368 x 216 mm [14 x 7 in.]). The beam was supported by bearing pads on steel plates centered at 38 mm (1.5 in.) from the beam ends.

The Phase I specimens were designed to resist a load of 17.8 kN (4 kips) with a $\phi = 0.75$. This led to a design load of 23.6 kN (5.3 kips). Pea-gravel concrete and small reinforcing

ACI Structural Journal, V. 104, No. 6, November-December 2007.
MS No. S-2006-333.R1 received August 21, 2006, and reviewed under Institute publication policies. Pertinent discussion including author's closure, if any, will be published in the September-October 2008 *ACI Structural Journal* if the discussion is received by May 1, 2008.

ACI member **M. Tyler Ley** *is an Assistant Professor at Oklahoma State University, Stillwater, OK. He received his BS from Oklahoma State University, and his MS and PhD from The University of Texas at Austin, Austin, TX. He is a member of ACI Committee 201, Durability of Concrete.*

ACI member **Kyle A. Riding** *is a PhD Candidate at the University of Texas at Austin. He received his BS from Brigham Young University, Provo, UT, and his MS from The University of Texas at Austin. He is a member of ACI Committee 201, Durability of Concrete.*

ACI member **Widianto** *is a Structural Engineer at Bechtel Corporation. He received his BS, MS, and PhD from the University of Texas at Austin. He is a member of ACI Committees 351, Foundations for Equipment and Machinery; 440, Fiber Reinforced Polymer Reinforcement; and Joint ACI-ASCE Committee 445, Shear and Torsion.*

ACI member **Sungjin Bae** *is a Postdoctoral Researcher at the University of Texas at Austin. He received his BS and MS from Hanyang University, Seoul, Korea, and his PhD from the University of Texas at Austin. He is a member of Joint ACI-ASCE Committee 441, Reinforced Concrete Columns.*

ACI Honorary Member **John E. Breen** *is the Nasser I. Al-Rashid Chair in Civil Engineering at the University of Texas at Austin. He is a member of ACI Committee 318, Structural Concrete Building Code, 318-B, Reinforcement and Development; 318-E, Shear and Torsion; and 355, Anchorage to Concrete.*

bars were used to construct the test specimens. A local ready mixed concrete company provided the concrete for the specimens. For design purposes, it was assumed that the concrete strength at testing was 24 MPa (3500 psi). The average compressive strength from 75 x 150 mm (3 x 6 in.) cylinders on the day of testing for Phase I was 21.8 MPa (3170 psi) with a standard deviation of 0.4 MPa (62 psi). The average splitting tensile strength for Phase I was 1.6 MPa (230 psi) with a standard deviation of 0.1 MPa (20 psi). The steel reinforcement used in Phase I consisted of 4 and 6 mm (0.16 and 0.24 in.) diameter deformed bars and 10- and 12-gauge smooth wires. The properties of the reinforcing steel for Phase I are summarized in Table 1.

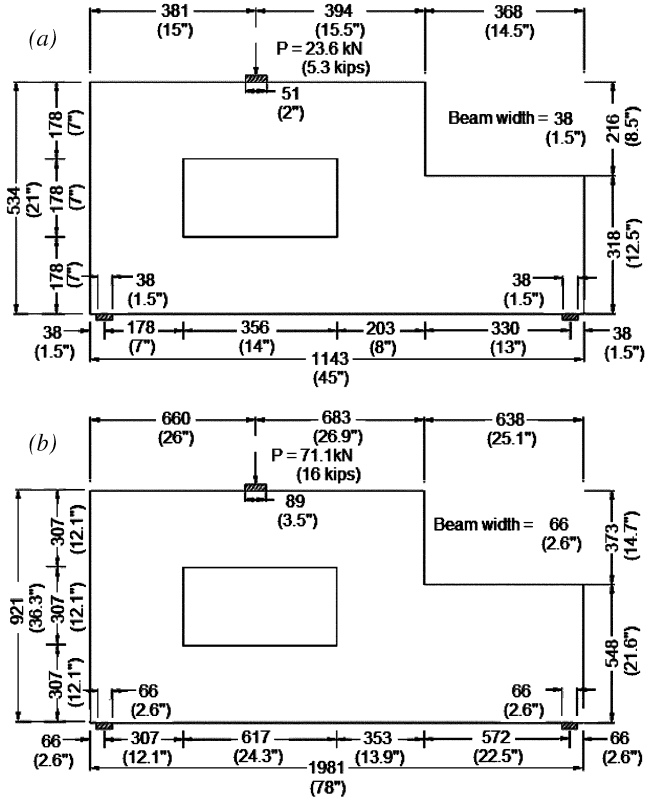

Fig. 1—Test specimen geometry: (a) Phase I; and (b) Phase II. (Dimensions are in mm [in.].)

Design process

Specimens 1 through 5 were independently designed by five groups of graduate students. Specimen 4i was a variation of Specimen 4. Specimen 6 was built with no reinforcement. Each reinforcing layout was designed using the strut-and-tie provisions in Appendix A of ACI 318-05 (ACI Committee 318 2005). Even though the same design provision was used for each specimen, the reinforcement design was quite different among the design teams.

As a first step in the design process, each group independently performed a two-dimensional finite-element analysis (FEA) to establish the elastic stress fields in the structure, as suggested by Schlaich et al. (1987) and Bergmeister et al. (1993). The use of FEA allows the designer to better understand the elastic stress fields in an unreinforced, uncracked member. The FEA for the specimen geometry and loading is shown in Fig. 2. Whereas the FEA can be useful to visualize the elastic flow of forces in the member, engineering judgment must be used for reinforcement design. After evaluating the performance requirements for the project, various teams designed their specimens to emphasize certain performance criteria. This emphasis had a large impact on the strut-and-tie model chosen by that team.

After a STM has been chosen, the strut-and-tie forces are calculated using a simple truss analysis. The reinforcing steel for the ties is then sized and the nodes and bearings are checked. Any concrete struts that are expected to carry high loads can be confined or reinforced to increase capacity. In bearing areas where a high compressive stress is anticipated, confinement steel may be provided to ensure that a local crushing failure of the concrete does not happen.

Table 1—Phase I reinforcing steel properties

Bar size	Area, mm^2 (in.^{2})	Yield strength, MPa (ksi)
6 mm ϕ	29 (0.045)	517 (75)
4 mm ϕ	12.2 (0.019)	565 (82)
10 gauge	10.6 (0.0165)	517 (75)
12 gauge	5.8 (0.009)	110 (16)

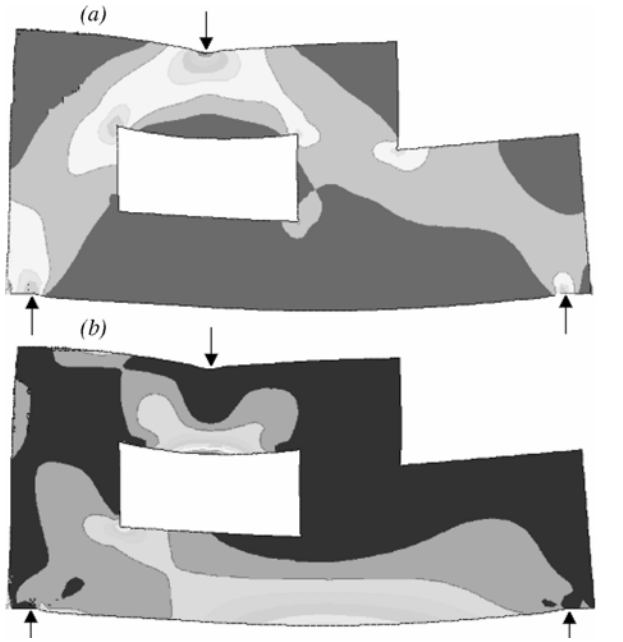

Fig. 2—Two-dimensional elastic finite element analysis: (a) first principal stress—compression; and (b) second principal stress—tension.

This design process was repeated several times until satisfactory models and steel layouts were found. The design teams often found that it was advantageous to use two overlapping models to efficiently distribute their reinforcing while keeping their truss models simple to analyze. This concept was presented by Schlaich et al. (1987) and has also been adopted in the FIP Recommendations 1996 (FIP Commission 3 1998) for deep beam design.

Specimen summary

Specimen 1 (Fig. 3)—The focus of this specimen was to carry the design load while minimizing the weight of reinforcement used. To accomplish this, the chosen STM attempted to minimize the length of ties used. It has been hypothesized by Schlaich et al. (1987) that minimizing the tie length results in the model with the lowest strain energy. To minimize the tie lengths most efficiently, the specimen was envisioned to behave as a tied arch with ties located at the bottom of the specimen and just above the opening. A tie was added in the dapped portion of the beam to ensure that the strut to the support did not fail. A tie was also added starting midlength at the bottom tie and extending diagonally to arrest any cracks that might extend from the corners of the opening to the bearing area. One V-shaped bar was added above the opening to help reinforce the struts needed under the point load. As mentioned previously, two STM were used to simplify the truss analysis and then superimposed. The steel reinforcement layout closely followed the ties chosen for the model. In all of the specimens in this paper, the reinforcing was placed at the middepth of the section, with any spirals used centered at middepth. Only 4 mm (0.16 in.) bars were used for this specimen as reinforcement. This specimen required 0.4 kg (0.9 lb) of steel; it initially cracked at 26.7 kN (6 kips) and failed at an ultimate load capacity of 40.5 kN (9.1 kips). The deflection at the point load at failure was 17 mm (0.66 in.). All deflections reported in this paper were measured at the point load. An efficiency rating was used to compare the specimen capacity with the weight of the steel cage used. The efficiency rating for this specimen was 101 kN/kg (10.1 kips/lb).

Specimen 2 (Fig. 4)—This specimen tried to distribute the external load around the opening by using a spreader beam that then transferred the load to a truss beam in the lower portion of the specimen. The steel reinforcement layout closely followed the ties in the model. To increase the capacity of the concrete struts in the spreader beam above the opening, 12-gauge wire was used in a spiral to provide confinement to the struts. The tie for the spreader beam was also extended to the edges of the specimen to arrest any cracks that might develop from the corners of the opening. Heads were welded to the reinforcing bar in this model to ensure all reinforcing bars were developed while using the minimum weight. This specimen required 1 kg (2.2 lb) of steel; it initially cracked at 22.2 kN (5 kips) and failed at an ultimate load capacity of 32.9 kN (7.4 kips). The failure mode for this specimen involved a combination of local crushing at the bearing and a stability failure. The specimen spalled under one side of the bearing plate. Under further loads, the specimen started to move laterally and the test was stopped. The deflection of this specimen at failure was 17.5 mm (0.69 in.). The efficiency rating for this specimen was 33 kN/kg (3.4 kips/lb).

Specimen 3 (Fig. 5)—The focus of this design was to provide a large amount of ductility while also meeting the strength requirements as the team wanted to ensure that they met the deflection requirements. To do this, the specimen was envisioned as a portal frame with a diagonal column on the dapped side, while totally neglecting the bottom portion of the beam. By taking this approach, the model ignores the flow of forces predicted by the FEA and instead chooses a model that forced a plastic hinge to form in a highly confined portion of the specimen. Stirrups were provided along the length of the envisioned frame to prevent a brittle failure. This specimen experienced very large cracking at design loads in the unreinforced area, but did provide more deflection at failure than any other specimen tested. This specimen used 1.04 kg (2.3 lb) of steel; it initially cracked at 22.2 kN (5 kips) and failed at an ultimate load capacity of 27.1 kN (6.1 kips). The deflection of this specimen at failure was 27.4 mm (1.08 in.). The efficiency rating for this specimen was 26 kN/kg (2.7 kips/lb).

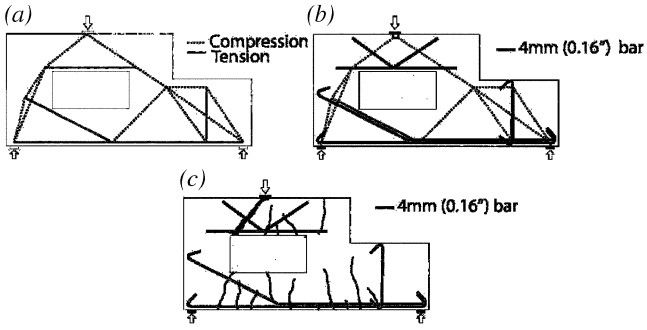

Fig. 3—Specimen 1: (a) STM; (b) reinforcing layout superimposed on STM; and (c) crack pattern at failure superimposed on reinforcing layout.

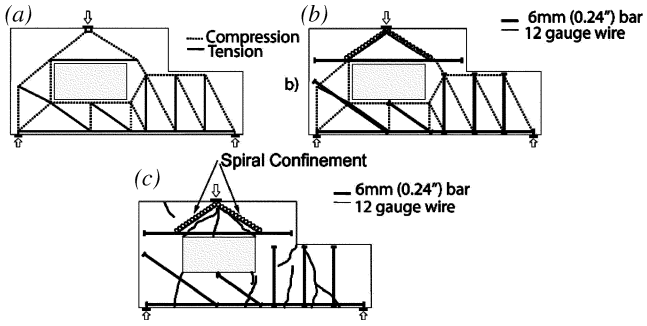

Fig. 4—Specimen 2: (a) STM; (b) reinforcing layout superimposed on STM; and (c) crack pattern at failure superimposed on reinforcing layout.

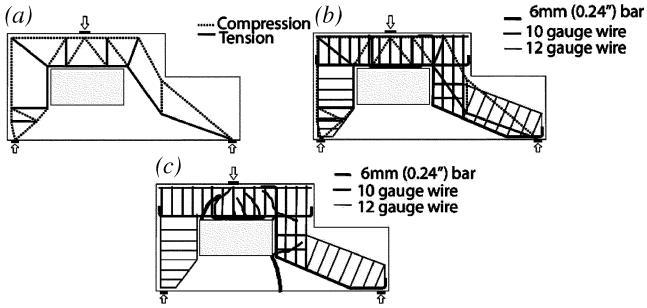

Fig. 5—Specimen 3: (a) STM; (b) reinforcing layout superimposed on STM; (c) crack pattern at failure superimposed on reinforcing layout.

Specimens 4 and 4i (Fig. 6 and 7)—In contrast to the previous specimen where the FEA was mostly ignored, this design team followed the FEA very closely when developing their STM. The model carries the load in the top portion of the member as a propped cantilever. This load is then brought to the reactions by a strut in the dapped side and a column at the cantilever reaction. A tie was provided in the bottom of the specimen to tie the two systems together. The primary reinforcement for the specimen was a 4 mm (0.16 in.) bar that ran from the reaction at the dapped side of the beam along the bottom to the other reaction, up the left side of the member, and then up to the top of the cantilever portion of the upper beam. The bar is then developed past the load point. Additional wire was used to provide confinement to the compression struts in the model. A spiral was used at the reaction on the nondapped side. This specimen used 1 kg (2.2 lb) of steel, it initially cracked at 28.5 kN (6.4 kips), and failed at an ultimate load capacity of 38.3 kN (8.6 kips).

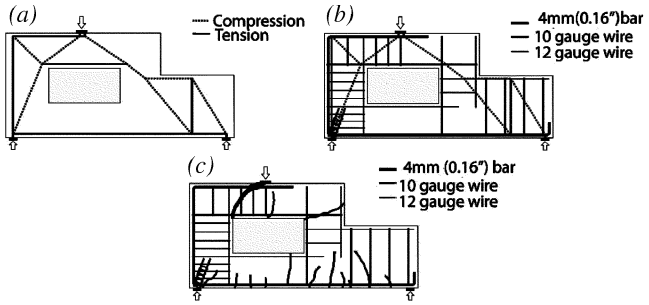

Fig. 6—Specimen 4: (a) STM; (b) reinforcing layout superimposed on STM; and (c) crack pattern at failure superimposed on reinforcing layout.

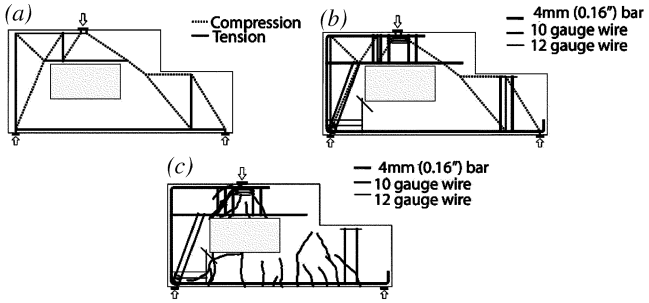

Fig. 7—Specimen 4i: (a) STM; (b) reinforcing layout superimposed on STM; and (c) crack pattern at failure superimposed on reinforcing layout.

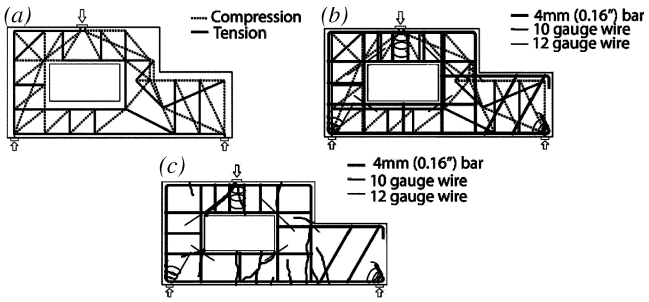

Fig. 8—Specimen 5: (a) STM; (b) reinforcing layout superimposed on STM; and (c) crack pattern at failure superimposed on reinforcing layout.

The deflection of this specimen at failure was 15.5 mm (0.61 in.). The efficiency rating for this specimen was 38 kN/kg (3.9 kips/lb). The failure mode for this specimen was a crushing of concrete under the load point that lead to an increased deflection in the joint to the right of the point load forming a flexural hinge. After investigating the failure, the team used the same strut-and-tie model and modified their reinforcing layout and tested the modified design. One major change was the increase in confinement provided under the load point. This redesign used 0.95 kg (2.1 lb) of steel. The specimen initially cracked at 28.5 kN (6.4 kips) and failed at an ultimate load capacity of 55.2 kN (12.4 kips). The deflection of this specimen at failure was 20.8 mm (0.82 in.). The efficiency rating for the redesigned specimen was 58 kN/kg (5.9 kips/lb). Details for the redesigned specimen are given in Fig. 7.

Specimen 5 (Fig. 8)—This design team attempted to create a STM that completely filled the boundaries of the member. Two models were made and then superimposed (as explained previously) to make the truss models easier to analyze. One model was designed to resist 1/3 of the external load while the other model was designed to resist the remaining 2/3. The primary load-resisting model used a truss to carry the loads throughout. The secondary load-resisting model used a design similar to Specimen 4. A strut was used on the dap end of the member and a cantilever and column were used for the other side. The results for these models were then combined and the reinforcing layout was designed primarily using 4 mm (0.16 in.) bars in an orthogonal grid along all openings. Wire reinforcing was used as confinement at both reactions and at the load point and also at all of the corners to arrest any cracks. This reinforcing layout was the most conventional of the design specimens. This specimen used 1.2 kg (2.7 lb) of steel, it initially cracked at 31.1 kN (7 kips) and failed at an ultimate load capacity of 42.7 kN (9.6 kips). The deflection of this specimen at failure was 18 mm (0.71 in.). The efficiency rating for this specimen was 36 kN/kg (3.6 kip/lb).

Specimen 6 (Fig. 9)—A plain concrete specimen was tested to find the capacity when relying only on the tensile strength of the concrete. This specimen failed at 18.7 kN (4.2 kips) with a deflection of 9.1 mm (0.36 in.). This was under the design load of 23.6 kN (5.3 kips) but was still higher than what was expected. One explanation for this is that the tensile strength of the concrete is typically assumed to be insignificant while using the STM. For the specimen scale used in this paper, this assumption may not be valid. The failed specimen is shown in Fig. 9.

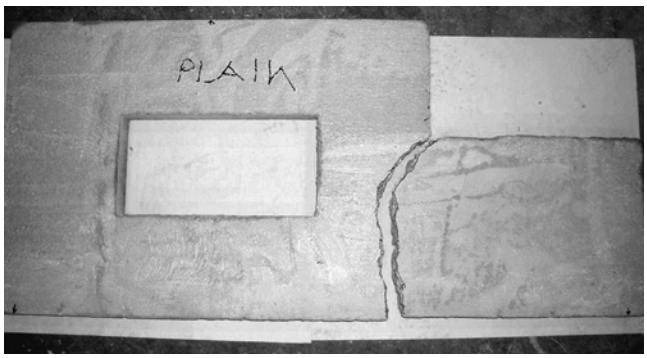

Fig. 9—Specimen 6 after failure.

Phase II testing

Two specimens were tested as part of the Phase II testing. The specimens were built using the same general geometry and loading pattern as the Phase I testing but adjusted for a larger scale. A reinforced specimen (Specimen 1) and a plain concrete specimen were tested at a larger scale. The specimen lengths used in Phase II of the testing were the same as that in Phase I multiplied by a scale factor (SF). The SF was calculated according to Eq. (1)

$$\text{SF} = \frac{\sqrt{A_t \times F_{yl}}}{A_s \times F_{ys}} \quad (1)$$

where SF is the specimen length scale factor, A_l is the large reinforcing bars' cross-sectional area, F_{yl} is the yield stress of the large reinforcing bars, A_s is the cross-sectional area of the small reinforcing bars, and F_{ys} is the yield stress of the small reinforcing bars (Zia et al. 1970). Six mm (0.24 in.) bars with a yield stress of 655 MPa (95 ksi) were used in the large specimen. The Phase II specimens were 1.73 times larger on the linear dimensions. This created a model whose scale was 1:6 from the original example problem. All truss member forces and the expected load-carrying capacity for the larger specimen is equal to the square of the scale factor or three times those in the small specimen.

The reinforced specimen that was part of Phase II of the testing was designed to resist a load of 53.4 kN (12 kips) with a $\phi = 0.75$. This resulted in a design load of 71.1 kN (16 kips). The beams were intended to be tested when the concrete compressive strength approximated that of the small specimens (21.8 MPa [3170 psi]). The measured compressive strength of the unreinforced concrete specimen was very close, at 21.1 MPa (3070 psi), with a standard deviation of 0.8 MPa (120 psi). The splitting tensile strength was 2.3 MPa (340 psi) with a standard deviation of 0.2 MPa (31 psi). The compressive strength of the reinforced specimen, however, was much higher, at 31.3 MPa (4540 psi), with a standard deviation of 1.2 MPa (179 psi). The splitting tensile strength was 3.2 MPa (470 psi) with a standard deviation of 0.1 MPa (20 psi).

Specimen 7—Specimen 7 was built using the same general reinforcement pattern as used in Specimen 1. However, 6 mm (0.24 in.) diameter reinforcing bars with a yield stress of 655 MPa (95 ksi) were used instead of the 4 mm (0.16 in.) diameter reinforcing bars that were used in Specimen 1. A similar cracking pattern was seen to the corresponding Phase I Specimen 1. Figure 10 compares the cracking patterns for Specimen 7 and Specimen 1. The ratio of failure load of the large specimen to small specimen was 2.9 for the reinforced specimen. This was very close to the predicted ratio of 3 and shows that the substantially higher concrete compressive strength had little effect. The reason the compressive strength difference did not affect the results is due to the specimens both failing by yielding of the steel. This specimen failed by first forming a crack parallel to the bottle strut to the left of the point load and then a final flexural hinge formed in the lower portion of the beam. The reinforcing steel in the lower portion of the beam yielded and fractured at the bottom of the beam at the intersection of the opening and the left column. This specimen used 1.8 kg (3.9 lb) of steel, cracked at 62.3 kN (14 kips) and failed at an ultimate load capacity of 117.4 kN (26.4 kips). The deflection of this specimen at failure was 28.1 mm (1.11 in.). The efficiency rating for this specimen was 65 kN/kg (6.8 kips/lb).

Specimen 8 (Fig. 11)—A plain concrete specimen with the same dimensions used in Specimen 7 was tested to see the effects of size on the failure mode and ultimate load capacity on the unreinforced specimen. This specimen fractured at a load of 36 kN (8.1 kips) and a deflection of 8.9 mm (0.35 in.). The ratio of failure load of the large specimen to small specimen was only 1.9 for the unreinforced specimen. The large unreinforced specimen also failed in completely different locations than the small unreinforced specimen, as shown in Fig. 12. This shows the unreliable structural behavior of unreinforced concrete. One area where this should not be overlooked is in the direction perpendicular to a compression strut. As shown in these tests, the tensile strength of the concrete should not be relied on to carry significant loads. Reinforcement should be added to carry the tensile stress in these regions.

EVALUATION OF TEST RESULTS

Specimens 1 through 5 and 7 carried more than the factored design load. A comparison between the specimens of the maximum load carried, efficiency rating, and deflection at failure is made in Table 2. Specimens 2 and 3 were the only reinforced members that cracked at a load lower than the design load. These specimens cracked at 94% of the design load, well above what would be expected for service conditions.

Figure 12 compares the load deflection response of the Phase I specimens. The graph shows a linear response up to the failure load on all except Specimen 3. The design of this specimen focused on providing a ductile failure. The deflection of this specimen increased linearly until the design load and then showed a softening with residual deflection and load-carrying capacity after ultimate load. Figure 13 compares the load deflection response for the Phase II specimens. Again, this graph shows a linear response up to the failure load.

The failure mode and final cracking patterns varied between the specimens. A graphical summary of the failure modes is presented in Fig. 14. One similarity was that each

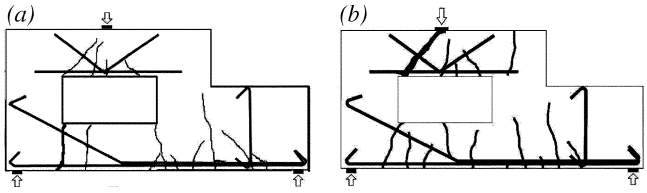

Fig. 10—(a) Cracking pattern of Specimen 7; and (b) cracking pattern of Specimen 1.

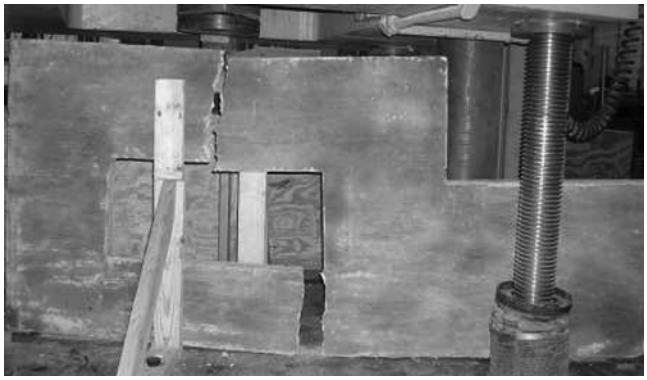

Fig. 11—Specimen 8 after failure.

mode of failure involved a shear failure also known as a bottle strut failure to the left of the point load. Next, a flexural hinge formed in the member and then a collapse mechanism was formed. This was the case for Specimens 1, 4, 4i, and 5. The flexural hinges all formed in different locations. The hinge location was typically due to the reinforcing layout used. The influence of the steel on the load redistribution and failure can be seen by examining the cracking patterns in Fig. 3 through 8 and 10. As stated previously, Specimen 2 failed due to stability after a bearing failure occurred under the load. Specimen 3 was designed as a portal frame without placing reinforcing below the opening. A fracture formed very early in the unreinforced section and the specimen failed once the shear hinge formed. This design team was able to achieve an increased ductility when compared with the other specimens from their reinforcement layout and proportioning. This method of performance-based design was used successfully in this example but should be used with caution as STM is only able to provide a safe, lower-bound design and is not able to predict stress redistribution or cracking locations. The unreinforced Specimen 6 failed as soon as a fracture formed in the lower portion of the member. The unreinforced Specimen 8 from Phase II simultaneously formed fractures in the upper and lower span.

The results of the large test shows the generality of small scale testing for STM with this geometry and load condition. Results also show that the size effect of adequately reinforced STM is minimal. These results confirm what other researchers have found that steel reinforcement allows for stress redistribution and for multiple cracks to form, and thus "a more gentle size effect may be expected in reinforced concrete members" (Shah et al. 1995).

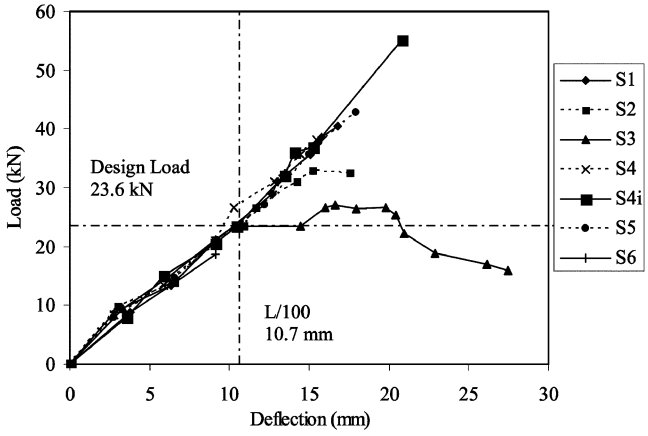

Fig. 12—Phase I load versus deflection curve (1 kN = 0.225 kips [25.4 mm = 1 in.]).

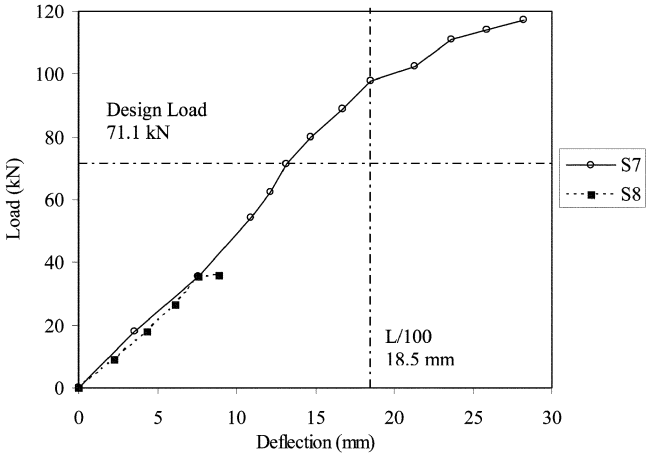

Fig. 13—Load deflection curves for Phase II testing (1 kN = 0.225 kips; 25.4 mm = 1 in.)

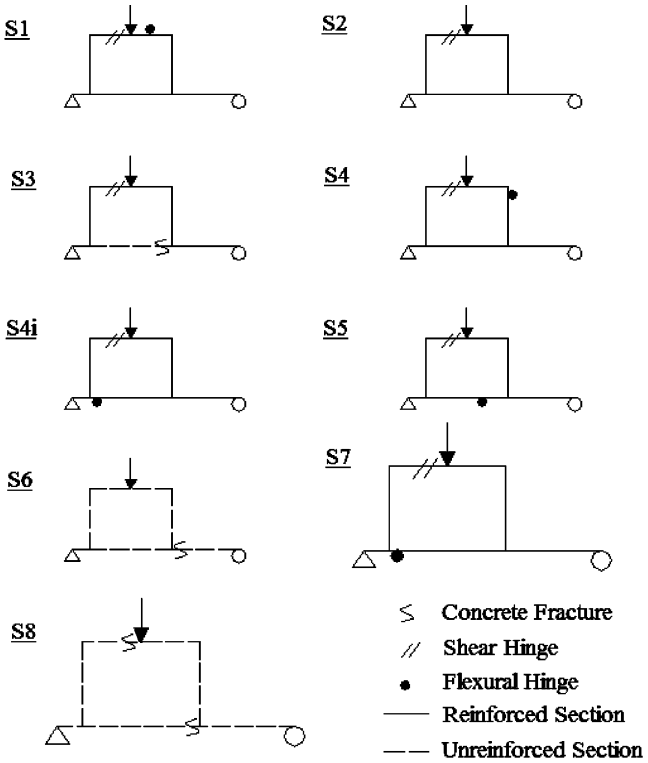

Fig. 14—Specimen failure modes.

Table 2—Summary of results

Phase	Specimen	Δ = *L*/100, mm (in.)	Δ at failure,* mm (in.)	P_u/ϕ, kN (kips)	Failure load, kN (kips)	Cracking load, kN (kips)	Efficiency, kN/kg (kips/lb)
I	S1	10.7 (0.42)	17 (0.66)	23.6 (5.3)	40.5 (9.1)	26.7 (6)	101 (10.1)
	S2	10.7 (0.42)	17.5 (0.69)	23.6 (5.3)	32.9 (7.4)	22.2 (5)	33 (3.4)
	S3	10.7 (0.42)	27.4 (1.08)	23.6 (5.3)	27.1 (6.1)	22.2 (5)	26 (2.7)
	S4	10.7 (0.42)	15.5 (0.61)	23.6 (5.3)	38.3 (8.6)	28.5 (6.4)	38 (3.9)
	S4i	10.7 (0.42)	20.8 (0.82)	23.6 (5.3)	55.2 (12.4)	28.5 (6.4)	58 (5.9)
	S5	10.7 (0.42)	18 (0.71)	23.6 (5.3)	42.7 (9.6)	31.1(7)	36 (3.6)
	S6	10.7 (0.42)	9.1 (0.36)	23.6 (5.3)	18.1 (4.2)	18.1 (4.2)	—
II	S7	18.5 (0.73)	28.1 (1.11)	71.1 (16)	117.4 (26.4)	62.3 (14)	65 (6.8)
	S8	18.5 (0.73)	8.9 (0.35)	71.1 (16)	36 (8.1)	36 (8.1)	—

*Deflection for all specimens were measured at load point.

CONCLUSIONS

Test results reported herein show that the STM developed by different designers varied substantially, which lead to reinforcing patterns that are in turn different and yet still yielded safe designs. Furthermore, strut-and-tie modeling offered the designer a flexibility to focus on performance design while also providing a safe design. Different performance criteria may be achieved with STM; however, the ultimate failure mode and load are not able to be predicted by STM. All reinforced strut-and-tie test specimens in this study carried loads greater than the factored design loads. The testing of a larger reinforced specimen showed that the scaled results were not dependant on the specimen size. This was not the case for the unreinforced specimens. The failure of the unreinforced specimens at different locations also shows the unreliable and variable nature of unreinforced concrete. Conservatism should be used whenever a structure is to rely on the tensile strength of concrete such as an unreinforced bottle strut. More full-scale tests are required on unreinforced configurations to determine their load capacity.

ACKNOWLEDGMENTS

The authors would to thank all of the individual members of the design teams for their contributions. Those individuals include M. Ahern, J. Argudo, M. Florea, K. Hampel, H. J. Kim, E. Koehler, T. Luthi, L. Mah, B. McBee, E. Mathvin, G. Mitchell, J. Norvell, I. Ornelas, S. Orton, P. Ruth, R. Tuchscherer, and D. Williams. The authors would also like to thank B. Stassney, M. Bell, and M. Rung for their assistance during the construction and testing of the specimens.

REFERENCES

ACI Committee 318, 2005, "Building Code Requirements for Structural Concrete (ACI 318-05) and Commentary (318R-05)," American Concrete Institute, Farmington Hills, MI, 430 pp.

Bergmeister, K.; Breen, J. E.; Jirsa, J. O.; and Kreger, M. E., 1993, "Detailing for Structural Concrete," *Research Report* 1127-3F, Center for Transportation Research University of Texas at Austin, Austin, TX, 300 pp.

Chen, B. S.; Hagenberger, M. J.; and Breen, J. E., 2002, "Evaluation of Strut-and-Tie Modeling Applied to Dapped Beams with Opening," *ACI Structural Journal*, V. 99, No. 4, July-Aug., pp. 445-450.

FIP Commission 3, 1998, "FIP Recommendation 1996, Practical Design of Structural Concrete," Fédération Internationale de la Precontrainte.

Maxwell, B. S., and Breen, J. E., 2000, "Experimental Evaluation of Strut and Tie Model Applied to Deep Beam with Opening," *ACI Structural Journal*, V. 97, No. 1, Jan.-Feb., pp. 142-148.

Muttoni, A.; Schwartz, J.; and Thurlimann, B., 1997, *Design of Concrete Structures with Stress Fields*, Birkhauser Verlag, Switzerland, 147 pp.

Reineck, K. H., ed., 2002, *Examples for the Design of Structural Concrete with Strut-and-Tie Models*, SP-208, American Concrete Institute, Farmington Hills, MI, 242 pp.

Schlaich, J.; Schäfer, K.; and Jennewein, M., 1987, "Toward a Consistent Design of Structural Concrete," *Journal of the Prestressed Concrete Institute*, V. 32, No. 3, May-June, pp. 74-150.

Shah, S. P.; Swartz, S. E.; and Ouyang, C., 1995, *Fracture Mechanics of Concrete: Applications of Fracture Mechanics to Concrete, Rock and Other Quasi-Brittle Materials*, John Wiley, New York, 591 pp.

Zia, P.; White, R. N.; and Vanhorn, D. A., 1970, "Principles of Model Analysis," *Models for Concrete Structures*, SP-24, American Concrete Institute, Farmington Hills, MI, 495 pp.